

# Self-consistent treatment of dynamics and chemistry in the winds from carbon-rich AGB stars. I. Tests of the equilibrium and kinetic chemical codes.

M. Pulecka<sup>1</sup>, M.R. Schmidt<sup>1</sup>, V.I. Shematovich<sup>2</sup>, and R. Szczerba<sup>1</sup>

<sup>1</sup> N. Copernicus Astronomical Center, Rabiańska 8, 87–100 Toruń, Poland

<sup>2</sup> Institute of Astronomy, Russian Academy of Sciences, Pyatnitskaya 48, Moscow, Russian Federation

Received; Accepted

## ABSTRACT

**Aims.** The main aim of the paper was performing test of our (chemical and kinetic) codes, which will be used during self-consistent modelling of dynamics and chemistry in the winds from C-rich AGB stars.

**Methods.** We use the thermodynamical equilibrium code to test the different databases of dissociation constants. We also calculate the equilibrium content of the gas using the kinetic code, which includes the chemical network of neutral–neutral reactions studied by Willacy & Cherchneff (1998). The influence of reaction rates updated using the UMIST database for Astrochemistry 2005 (UDFA05), was tested.

**Results.** The local thermodynamical equilibrium calculations have shown that the NIST database reproduces fairly well equilibrium concentrations of Willacy & Cherchneff (1998), while agreement in case of Tsuji (1973) dissociation constants is much worse.

The most important finding is that the steady state solution obtained with the kinetic code for reaction network of Willacy & Cherchneff (1998) is different from the thermodynamical equilibrium solution. In particular, CN and C<sub>2</sub>, which are important opacity sources are underabundant relative to thermodynamical equilibrium, while O-bearing molecules (like SiO, H<sub>2</sub>O, and OH) are overabundant. After updating the reaction rates by data from the UDFA05 database consistency in O-bearing species becomes much better, however the disagreement in C-bearing species is still present.

**Key words.** astrochemistry – stars: AGB – stars: carbon – stars: atmospheres, stars: kinematic – stars : circumstellar matter – stars: winds, outflows

## 1. Introduction

Asymptotic Giant Branch (AGB) stars develop a molecular dusty wind, driven by radiation pressure on dust grains condensating in the warm molecular layers. The new formed molecules and dust are deposited then into interstellar medium (ISM) and contribute to the global matter budget of galaxies. Therefore, the determination of molecular and dust contents in the AGB winds is important for understanding of their further re-processing in the ISM before, eventually, matter ends up in a new star forming regions.

Chemical evolution of gas around AGB stars takes place at such different conditions like thermodynamical equilibrium in stellar photospheres, non-equilibrium (including possible shock-induced) chemistry, dust formation and photon dominated chemistry in circumstellar envelopes.

Observations of circumstellar envelopes at infrared and millimetre range demonstrate that they are very rich in molecules. In the case of the well-studied C-rich AGB star IRC+10216 the number of identified molecules exceeded 60 (Olofsson 2006). The majority of the observed molecules are carbon-chain molecules such as the cyanopolynes, the hydrocarbon radicals and carbenes, as well as organo-sulphur and organo-silicon molecules. Interferometric and single dish observations show that carbon-chain molecules are distributed in the hollow shells around central star. Such distribution has been interpreted as arising from photochemistry of parent molecules (e.g. C<sub>2</sub>H<sub>2</sub> and HCN) flowing away from the star (see

e.g. reviews by Glassgold 1996; Millar 2003). The new space and ground-based projects (e.g. Stratospheric Observatory for Infrared Astronomy – SOFIA, The Atacama Large Millimeter Array – ALMA or Herschel Space Observatory) will allow us to investigate the circumstellar molecular inventory in much more details by using, not yet fully exploited, sub-millimetre range.

With the aim to prepare tools for analysing the new sub-millimetre observations of AGB stars we are in a process of developing a self-consistent treatment of dynamics and chemistry in the circumstellar envelopes. The first effort to build the chemical network of reactions for conditions close to thermodynamical equilibrium (high density and temperature) in C-rich environment was done by Willacy & Cherchneff (1998) (hereafter WC98). Since the considered densities are high and effective temperature of the star is low, only neutral–neutral bimolecular and termolecular reactions were considered. WC98 investigated chemistry of sulphur and silicon in the inner wind of IRC+10216. Their non-equilibrium calculations started from chemical composition derived at the local thermodynamical equilibrium (LTE) conditions. It was found that the parent molecules C<sub>2</sub>H<sub>2</sub> and CO are unaffected by the shocks, but the abundances of daughter molecules can be significantly altered by the shock-driven chemistry. Their model indicated that molecule production by the shock-driven chemistry close to the photosphere can be significantly more important than the LTE chemistry. Recently, Cherchneff (2006) investigated the chemistry and composition of the quasi-static molecular layers

of AGB stars using the same semi-analytical model of shock dynamics as in WC98.

In modelling of stellar atmospheres it is commonly assumed that conditions of local thermodynamical equilibrium prevails. Molecular content is then defined by dissociation constants. In the outflow, in the presence of shocks, kinetic equations must be solved for some chemical network. When local thermodynamical equilibrium is valid, at some position in the stellar atmosphere, both approaches should produce the same molecular concentrations. If not, then an inconsistency will appear, darkening the interpretation of obtained results. The aim of our paper is to clarify this point for future application of available chemical networks in the non-equilibrium computations of chemistry in the inner layers of carbon-rich outflows.

In this paper we present our steady-state chemical code and test (some of) the available chemical databases using for comparison work of WC98. In the next paper (Schmidt et al. in preparation) we will discuss our approach to self-consistent treatment of dynamics and chemistry. The first preliminary results of such computations were presented by Pulecka et al. (2005a) (using the TITAN hydrodynamical code) and Pulecka et al. (2005b) (using the FLASH hydrodynamical code).

## 2. Test of chemical codes: The thermodynamical equilibrium

In the stellar photospheres the dynamical timescales are much longer than the timescales of molecular formation (Glassgold 1996). Therefore, to determine local molecular contents it is sufficient to apply the thermodynamical equilibrium (TE) conditions. To compute molecular composition in the local TE conditions one needs to know the temperature ( $T$ ), the total gas number density ( $n$ ), or equivalently the total gas pressure ( $p$ ), and the initial elemental abundances. We have constructed such TE code and present results of the performed tests.

### 2.1. The thermodynamical equilibrium code

The equilibrium chemistry code is based on the Russell's (Russell 1934) approach. This method uses the fictitious pressure  $p_f(X)$ , which is the pressure exerted by element X if all the gas were in the neutral form of the atomic species X. Hence the fictitious pressure of element X is given by:

$$p_f(X) = p_X + \sum_Y \alpha_{X,Y} p_Y, \quad (1)$$

where:  $p_Y$  – partial pressure<sup>1</sup> of molecular species Y, which contains element X,  $\alpha_{X,Y}$  – the stoichiometric coefficient indicating the number of element X involved in molecule Y. For example, in the case of hydrogen we have:

$$p_f(H) = p_H + 2p_{H_2} + p_{CH} + 2p_{CH_2} + \dots \quad (2)$$

(plus all examined hydrogen-bearing molecules).

Partial pressure of compound X is related to its concentration  $n_X$  [ $\text{cm}^{-3}$ ] by the ideal gas law  $p_X = n_X k T$  [ $\text{dyn cm}^{-2}$ ], where  $k$  – Boltzmann constant [ $\text{erg/K}$ ], and  $T$  – temperature [ $\text{K}$ ]. Using

<sup>1</sup> The partial pressure of species Y is the pressure of the gas if no other species were presented in the medium.

the partial pressures, the dissociation constant ( $K_p$ ) of molecule AB ( $AB \rightarrow A + B$ ) can be expressed as:

$$K_p(AB) = \frac{p_A p_B}{p_{AB}} = \frac{n_A k T n_B k T}{n_{AB} k T} = \frac{n_A n_B}{n_{AB}} k T, \quad (3)$$

where:  $p_A, p_B, p_{AB}$  – partial pressures of atoms A, B, and molecule AB,  $n_A, n_B, n_{AB}$  – their concentrations. Therefore by employing the Eq. 3, the fictitious pressure of hydrogen can be rewritten to:

$$p_f(H) = p_H + 2 \frac{p_H^2}{K_p(H_2)} + \frac{p_H p_C}{K_p(CH)} + 2 \frac{p_H^2 p_C}{K_p(CH_2)} + \dots \quad (4)$$

Note, that dissociation constants can be determined from the differences of the corresponding Gibbs free energies<sup>2</sup> Since, the fictitious pressure reflects the conservation of mass for element X, then  $p_f(X)$  for any other atomic species X can be expressed in terms of the fictitious pressure of hydrogen  $p_f(H)$ :

$$p_f(X) = A(X) p_f(H), \quad (6)$$

where:  $A(X) = \frac{n_X}{n_H}$  is abundance of element X relative to hydrogen.

To close this set of nonlinear equations for fictitious pressures we need only the equation for the total gas pressure, which is obtained by summing the partial pressures of all examined species. This final set of equations is solved using the Newton-Raphson's method. The solution gives the partial pressure of atoms, which are used then to calculate molecular partial pressures (i.e. in fact their concentrations) by employing Eq. 3.

### 2.2. The equilibrium case of WC98

In a first test of our thermodynamical equilibrium code we aimed to reproduce the thermodynamical equilibrium concentrations of species given in Table 3 of WC98. This table contains equilibrium abundances determined at distance of  $1.2 R_*$  and physical conditions specified in the 1<sup>st</sup> entry of their Table 2 ( $T = 2062$  [K] and  $n = 3.68 \times 10^{14}$  [ $\text{cm}^{-3}$ ] what corresponds to  $p = 1.05 \times 10^2$  [ $\text{dyn cm}^{-2}$ ]). To reproduce the equilibrium molecular content at these conditions we need to know the initial elemental abundances and the dissociation constants.

The initial elemental abundances were determined by summing abundances of all species (see Table 3 of WC98) containing a given element. The obtained values are given in Col. 2 of Table 1, where abundance of element X is given by  $\epsilon(X) = \log \frac{n_X}{n_H} + 12$ , and  $n_X$  is concentration of element X. For comparison, the solar abundances of H, He, C, O, N, Si, and S from Grevesse & Sauval (1998) (hereafter GS98) and Asplund et al. (2005) (hereafter A05) are shown in Cols. 3 and 4, respectively. The initial element abundances assumed by WC98 are essentially solar ones except of C/O ratio, which was assumed to be about 1.5.

<sup>2</sup> Here the sign  $^\circ$  marks conditions when temperature is 273.15 K and the absolute pressure is 1 atm (i.e. 1.01325 bar,  $1.01325 \times 10^6$  [ $\text{dyn cm}^{-2}$ ], 101.325 [kPa]). ( $\Delta G^\circ$ ) of products (A, B) and reactant (AB) according to:

$$K_p(AB) = C^{\Delta v} \exp\left(-\frac{\Delta G^\circ}{RT}\right), \quad (5)$$

where:  $R = 8.32441 \times 10^7$  [ $\text{erg K}^{-1} \text{mol}^{-1}$ ] is the ideal gas constant,  $C = 1.01325 \times 10^6$  [ $\text{dyn cm}^{-2}$ ] and  $\Delta v$  is the stoichiometric factor of a given dissociation reaction.

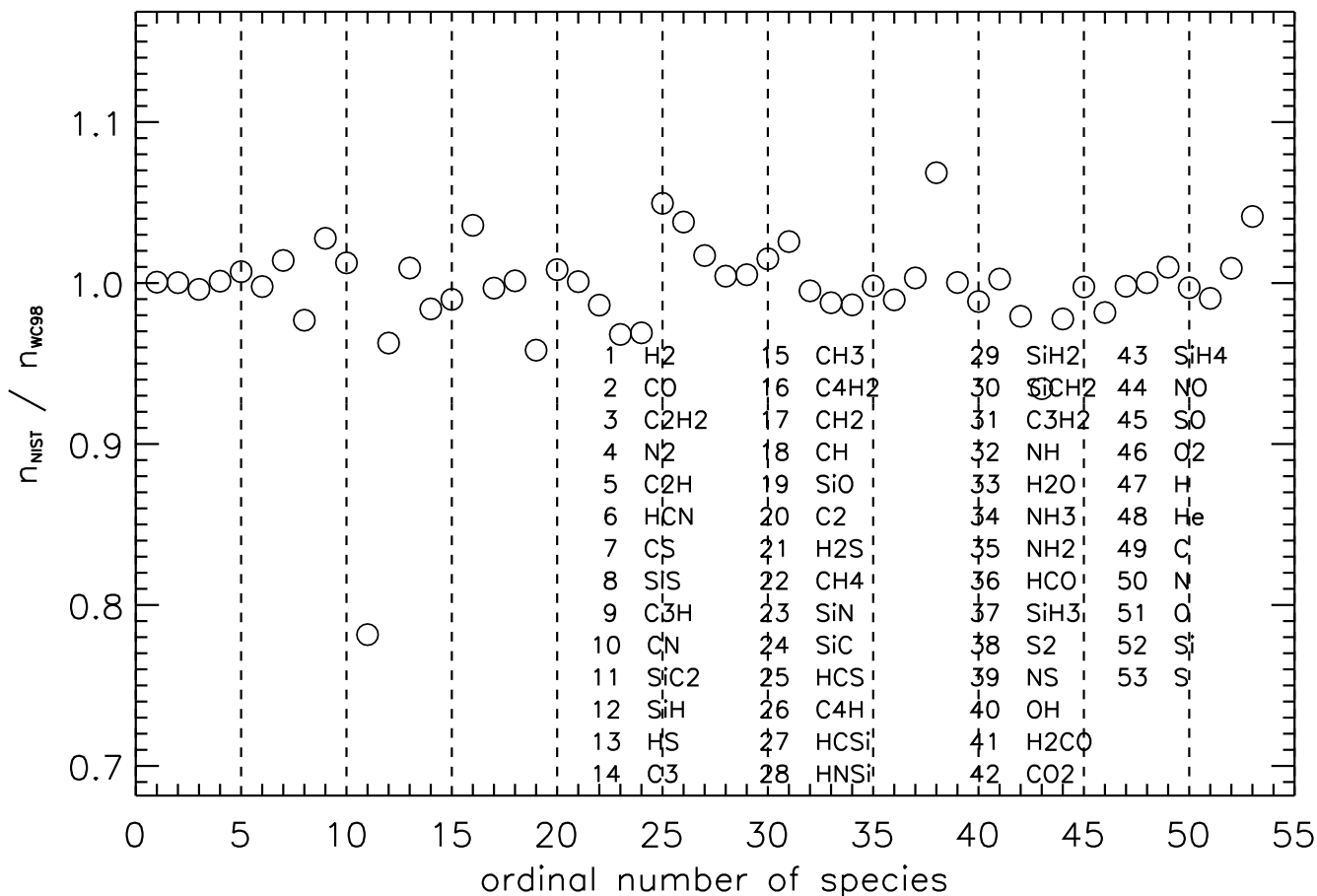


**Fig. 1.** The ratio of NIST and WC98 equilibrium concentrations. The order of species (except of elements, which are placed at the right side of the figure) follows decreasing concentrations of WC98.

**Table 1.** The initial abundances of elements:  $\epsilon(X) = \log \frac{n_X}{n_H} + 12$ .

element (1)	WC98 (2)	GS98 (3)	A05 (4)
H	12.00	12.00	12.00
He	10.99	10.93	10.93
C	8.98	8.56	8.39
N	8.06	8.05	7.78
O	8.79	8.93	8.66
Si	7.49	7.55	7.51
S	7.19	7.33	7.14

The dissociation constants were obtained using species concentrations given in Table 3 of WC98 by employing Eq. 3. Note that the dissociation constants derived in such a way are valid *only* for the conditions (temperature) specified above. As expected, with such  $K_p$ 's and initial elemental abundances given in column 1 of Table 1, the obtained equilibrium concentrations are in a very good agreement with values given in Table 3 of WC98. However, after discussion with K. Willacy, we realized that there are some misprints for the concentrations of  $C_2$  and  $SiH_4$  in Table 3 of WC98. Therefore, during further computation we have implemented the original  $\Delta G^\circ$ 's (kindly provided by K. Willacy) from work of WC98. These  $\Delta G^\circ$ 's are collected now in Table 2 (Cols. 3 and 8), and were used to determine equilibrium

species concentrations which will be referred hereafter as WC98 concentrations. The molecules listed in this table (with ordinal numbers in Cols. 1 and 6) are organised in order of decreasing WC98 concentrations.

### 2.3. Comparison of TE concentrations based on WC98, NIST and Tsuji databases

As was described in Sect. 2.2 determination of TE concentrations at specified conditions requires knowledge of  $K_p$ 's (or equivalently  $\Delta G^\circ$ 's). The most comprehensive database, which is publicly available and allows to compute dissociation constants is that collected by the National Institute of Standards and Technology (NIST). The NIST chemistry WebBook<sup>3</sup> provides thermochemical data, like enthalpy of formation ( $H^\circ$ ) and molar entropy ( $S^\circ$ ) for different temperatures at standard conditions. These quantities allow determination of the Gibbs free energy ( $G^\circ$ ) for all examined species according to:

$$G^\circ = H^\circ - T S^\circ. \quad (7)$$

Thus, we can determine the difference of Gibbs free energies ( $\Delta G^\circ$ ) for products and reactants, of the direct dissociation of

<sup>3</sup> <http://webbook.nist.gov/chemistry/>

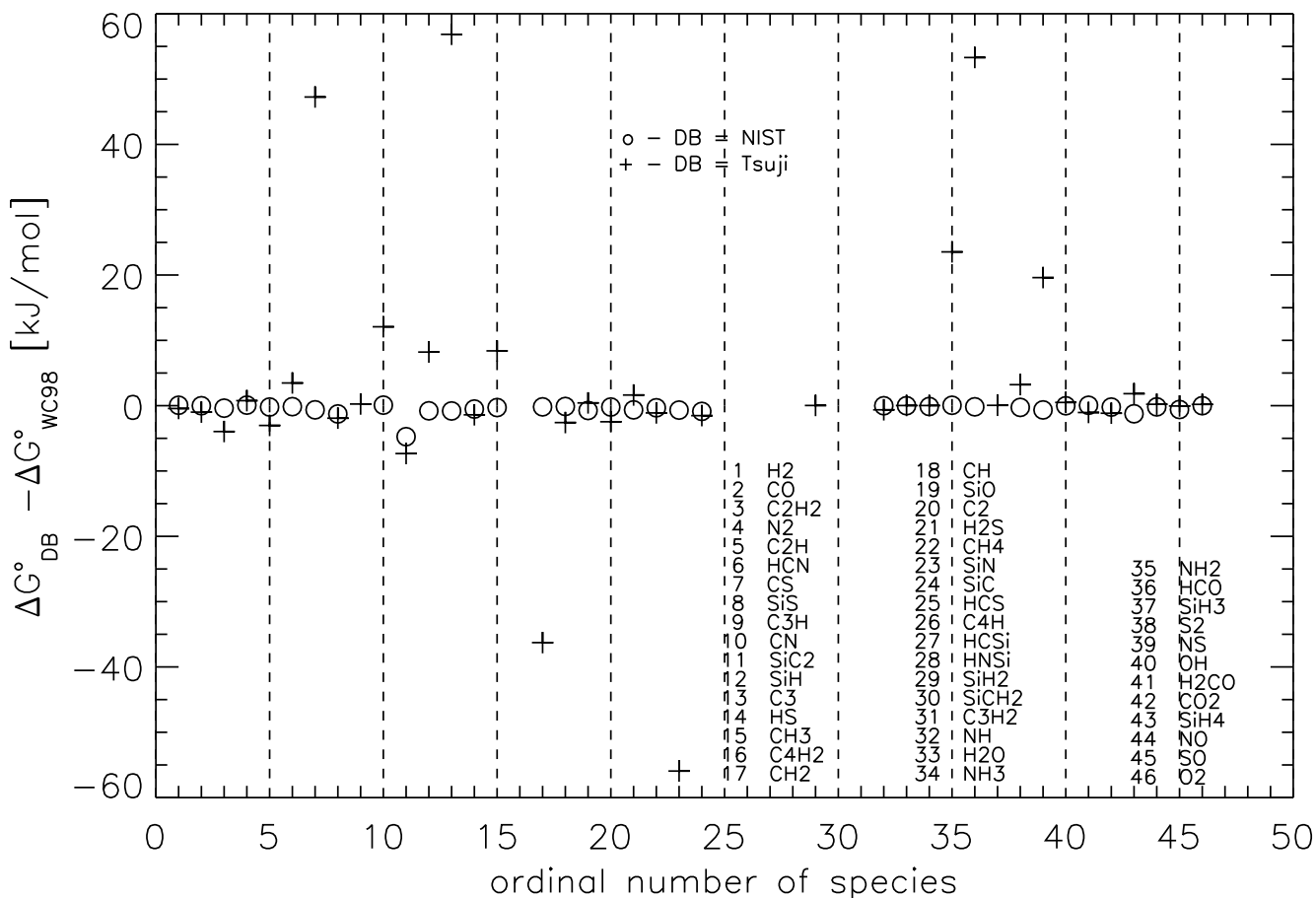


**Fig. 2.** The differences of  $\Delta G^\circ$  between database (DB: DB = NIST or Tsuji) and WC98. Results are marked by circles for the NIST database and by pluses for the Tsuji database. The order of species is same as in Fig. 1

molecule into single atoms, and use them to find the dissociation constants from Eq. 5.

We computed concentrations of species according to the method described in Sect. 2.1, using the dissociation constants obtained from the NIST database for  $T = 2062$  [K]. The NIST database does not contain thermochemical data for some molecules:  $C_3H$  - #9 (number appearing after symbol # is the ordinal number of a given molecule used in Fig. 1),  $C_4H_2$  - #16,  $HCS$  - #25,  $C_4H$  - #26,  $HCSi$  - #27,  $HNSi$  - #28,  $SiH_2$  - #29,  $SiCH_2$  - #30,  $C_3H_2$  - #31,  $SiH_3$  - #37, so we have used  $\Delta G^\circ$ 's from WC98, instead. The comparison between NIST and WC98 concentrations is shown in Fig. 1. The order of species (except of elements, which are placed at the right side of the figure) follows decreasing concentrations of WC98. The consistency is fairly good (almost all results agree within about 7 %, with the exception of  $SiC_2$  - #11 concentration, for which difference is about 22 %).

From chemical point of view a better illustration of discrepancies between different databases of thermochemical data is comparison between  $\Delta G^\circ$ 's. Therefore, in Cols. 4 and 9 of Table 2 we provide the  $\Delta G^\circ$ 's derived from the NIST database. We left empty spaces for species with missing data in that database. In Fig. 2 we plotted the differences between  $\Delta G^\circ$ ' from NIST and WC98 (circles) for each species. Again, the order of species (except of elements, which are placed at

the right side of the figure) follows decreasing concentrations of WC98. For molecules without data in the NIST database there are no corresponding symbols in Fig. 2. As one can see energies agrees within about 2 [kJ mol<sup>-1</sup>] with exception of  $SiC_2$  for which discrepancy is about 5 [kJ mol<sup>-1</sup>]. Another widely used database, especially in the modelling of stellar atmospheres, is the set of dissociation constants compiled by Tsuji (1973). The thermal dependence of  $K_p$ 's in this database is given by:

$$\log K_p = c_0 + c_1\theta + c_2\theta^2 + c_3\theta^3 + c_4\theta^4, \quad (8)$$

here:  $c_{i,i=0,1,\dots,4}$  - are coefficients derived by Tsuji and  $\theta = \frac{5040}{T}$ . This equation allow us to compute dissociation constants at the temperature of interest ( $T = 2062$  K). The corresponding  $\Delta G^\circ$ 's, computed from Eq. 5, are collected in Cols. 5 and 10 of Table 2, and compared with WC98 and NIST values in Fig. 2 (pluses). The Tsuji's database does not contain seven molecules among 46 considered:  $C_4H_2$  - #16,  $HCS$  - # 25,  $C_4H$  - #26,  $HCSi$  - #27,  $HNSi$  - #28,  $SiCH_2$  - #30, and ,  $C_3H_2$  - #31 (empty spaces in Table 2, and in Fig. 2). In general, agreement between  $\Delta G^\circ$ 's from Tsuji and WC98 is worse than that in case of NIST. The largest differences are seen for:  $CS$  - #7,  $CN$  - #10,  $SiC_2$  - #11,  $SiH$  - #12,  $C_3$  - #13,  $CH_3$  - #15,  $CH_2$  - #17,  $SiN$  - #23,  $NH_2$  - #35,  $HCO$  - #36, and  $NS$  - #39.  $\Delta G^\circ$ 's for other molecules differ less than about 4 [kJ/mol].

**Table 2.**  $\Delta G^\circ$  in [kJ/mol] for  $T = 2062$  K and  $p = 1$  atm in case of WC98, NIST, and Tsuji (1973).

#	species	WC98	NIST	TSUJI	#	species	WC98	NIST	TSUJI
(1)	(2)	(3)	(4)	(5)	(6)	(7)	(8)	(9)	(10)
1	H <sub>2</sub>	207.6	206.1	205.6	24	SiC	215.4	214.5	213.9
2	CO	801.6	801.6	800.6	25	HCS	463.0		
3	C <sub>2</sub> H <sub>2</sub>	878.4	878.0	874.4	26	C <sub>4</sub> H	1279.8		
4	N <sub>2</sub>	684.3	684.4	685.1	27	HCSi	386.0		
5	C <sub>2</sub> H	676.0	675.8	673.0	28	HNSi	476.7		
6	HCN	770.0	769.8	773.5	29	SiH <sub>2</sub>	150.4		150.4
7	CS	453.8	453.2	501.1	30	SiCH <sub>2</sub>	555.8		
8	SiS	372.7	371.4	370.8	31	C <sub>3</sub> H <sub>2</sub>	1038.2		
9	C <sub>3</sub> H	1049.7		1050.0	32	NH	109.9	109.9	109.3
10	CN	507.0	507.1	519.1	33	H <sub>2</sub> O	455.4	455.4	455.4
11	SiC <sub>2</sub>	740.9	736.2	733.6	34	NH <sub>3</sub>	464.7	464.6	464.7
12	SiH	94.8	94.0	103.0	35	NH <sub>2</sub>	277.1	277.2	300.6
13	C <sub>3</sub>	794.3	793.5	851.1	36	HCO	662.7	662.5	716.0
14	HS	152.5	152.0	151.1	37	SiH <sub>3</sub>	280.9		281.0
15	CH <sub>3</sub>	516.5	516.2	524.9	38	S <sub>2</sub>	183.7	183.4	186.9
16	C <sub>4</sub> H <sub>2</sub>	1550.3			39	NS	262.4	261.7	282.0
17	CH <sub>2</sub>	318.8	318.6	282.5	40	OH	212.1	212.1	212.6
18	CH	131.7	131.6	129.1	41	H <sub>2</sub> CO	763.3	763.4	762.3
19	SiO	537.6	536.9	538.0	42	CO <sub>2</sub>	1024.3	1024.1	1023.1
20	C <sub>2</sub>	346.4	346.2	343.9	43	SiH <sub>4</sub>	335.1	333.9	336.9
21	H <sub>2</sub> S	286.8	286.2	288.4	44	NO	395.5	395.3	395.7
22	CH <sub>4</sub>	667.7	667.4	666.6	45	SO	279.3	278.7	279.2
23	SiN	317.3	316.6	261.4	46	O <sub>2</sub>	234.8	234.8	235.0

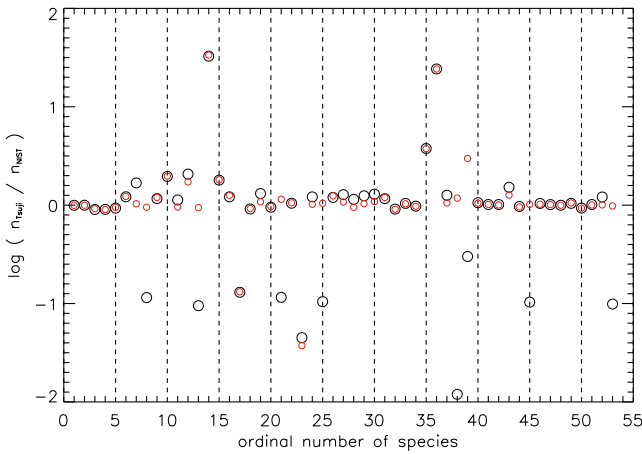


**Fig. 3.** The ratio between Tsuji and NIST equilibrium concentrations at conditions specified in Sect. 2.2 – black circles. Red circles mark the ratio, when  $\Delta G^\circ$  for CS in the Tsuji database was replaced by the value from WC98. The order of species is same as in Fig. 1

The influence of differences between the Tsuji and NIST  $\Delta G^\circ$ 's on species concentration can be seen in Fig. 3<sup>4</sup> – black circles. The order of species is same as in Fig. 1. We plotted there the logarithm of Tsuji concentrations relative to those of NIST (using the WC98 values of  $\Delta G^\circ$  in case of molecules with missing data). The consistency is rather poor. Concentrations for all molecules with considerable discrepancies in  $\Delta G^\circ$ 's are significantly different, but additionally some other species reached well different equilibrium state. For example, for all sulfur-bearing species, except of CS – #7 (i.e. SiS – #8, HS – #14, H<sub>2</sub>S – #21, HCS – #25, S<sub>2</sub> – #38, NS – #39, SO – #45, S – #53), we see very large discrepancies (even by factor of 84! for S<sub>2</sub>), in spite of the fact that differences between  $\Delta G^\circ$ 's are significant only in case of CS and NS. Among other molecules with significant discrepancy in concentrations are

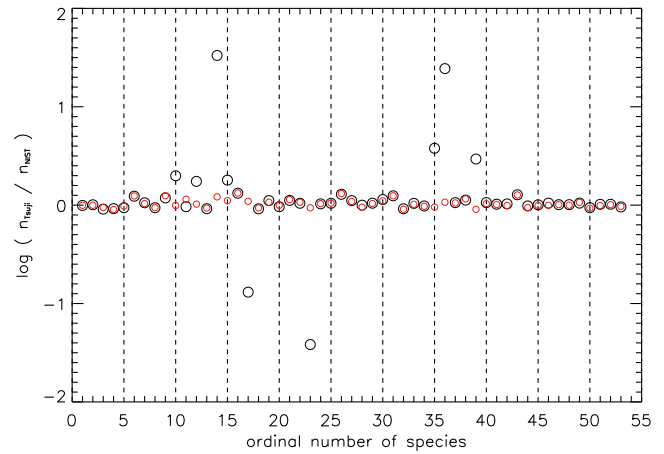


**Fig. 4.** The ratio between Tsuji (with  $\Delta G^\circ$  for CS replaced by the value from NIST) and NIST equilibrium concentrations at conditions specified in Sect. 2.2 – black circles. Red circles mark the ratio, with additional replacement of  $\Delta G^\circ$  for CS, CN, SiC<sub>2</sub>, SiH, C<sub>3</sub>, CH<sub>3</sub>, CH<sub>2</sub>, SiN, NH<sub>2</sub>, HCO, and NS in the Tsuji database by the values from WC98. The order of species is same as in Fig. 1

those containing C: C<sub>3</sub> – #13, CH<sub>2</sub> – #17 and HCO – #36; two silicon-bearing molecules: SiN – #23 and SiH – #12; and radical NH<sub>2</sub> – #35.

#### 2.4. The influence of changes in the $\Delta G^\circ$ 's on the TE concentrations

Here we test the influence of changes in  $\Delta G^\circ$  on equilibrium molecular content of examined gas.

In the first test we only replaced the Tsuji  $\Delta G^\circ$  for CS (this molecule has the largest equilibrium concentration among S-bearing molecules) by the smaller value from the NIST database. The correlation between the Tsuji and NIST concentrations becomes much better (see red circles in Fig. 3<sup>4</sup>),

<sup>4</sup> Figs.3–5 and 7 are available only in the online version.

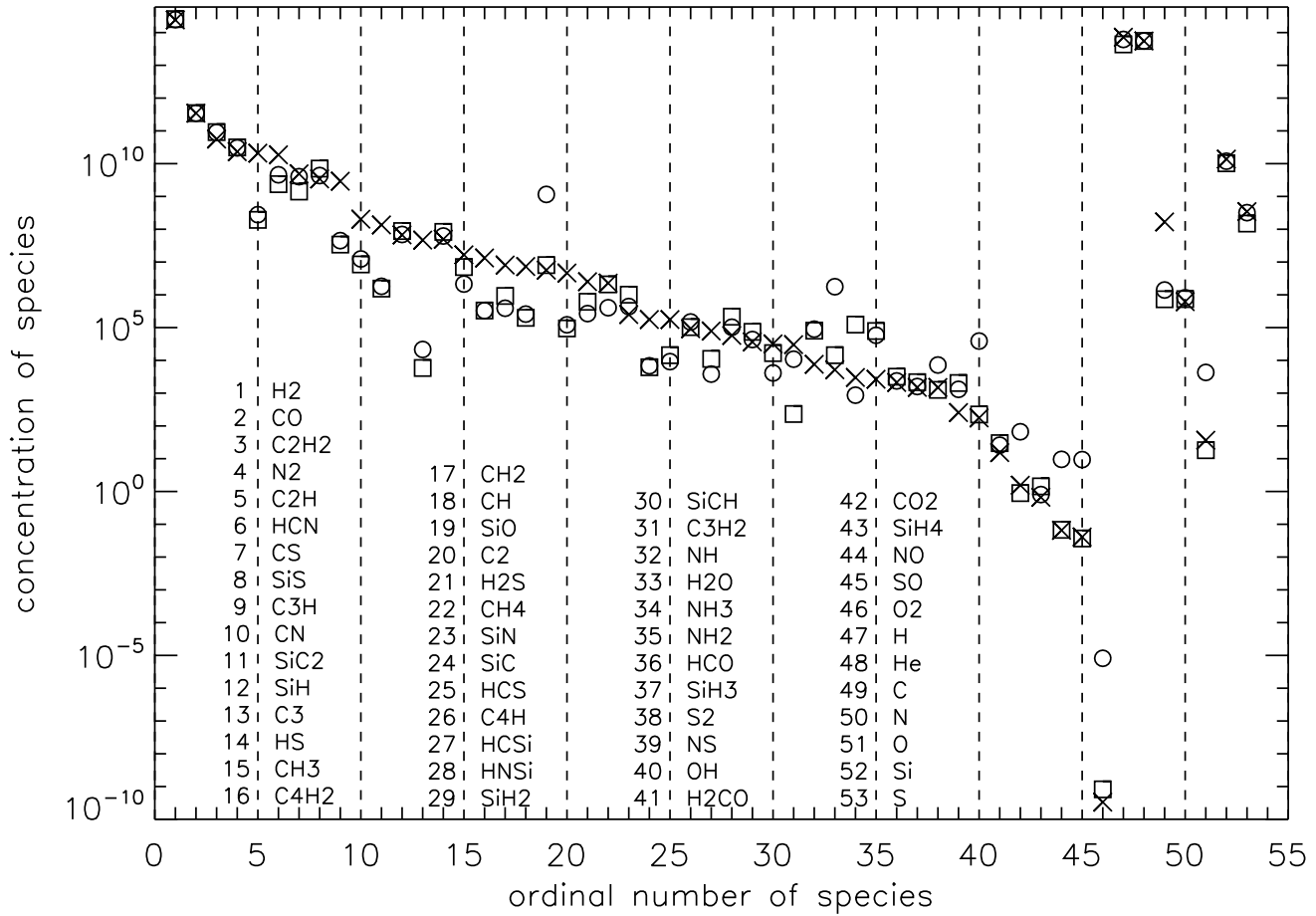


**Fig. 6.** Comparison between species concentrations in  $[\text{cm}^{-3}]$  derived by our kinetic code for case 1 – crosses, and for case 2 – circles, at conditions specified in the 1<sup>st</sup> entry of Table 2 in WC98. Squares mark concentration for case 2, with rate constants updated using the UDFA05 database. The order of species is same as in Fig. 1.

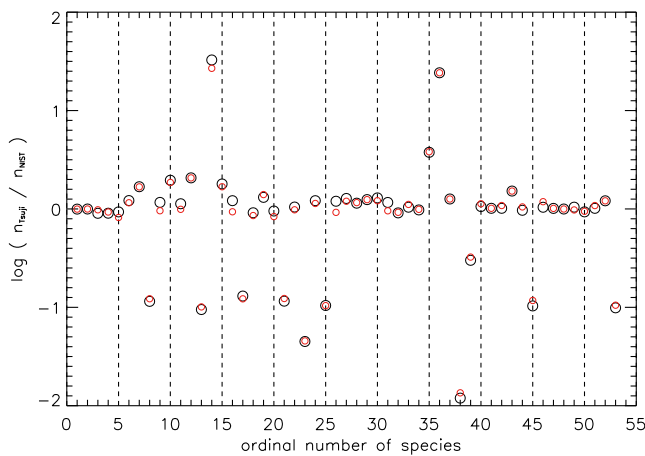


**Fig. 5.** The ratio between Tsuji and NIST equilibrium concentrations at conditions specified in Sect. 2.2 – black circles. Red circles mark the ratio, when  $\Delta G^\circ$  for  $\text{C}_2\text{H}_2$  in the Tsuji database was replaced by the value from NIST. The order of species is same as in Fig. 1

especially for family of all S-bearing molecules. Decrease in concentration of CS – #7 releases atomic carbon and sulfur, and the excess of sulfur increases concentrations of all S-bearing species. However at the same time, the increase in SiS – #8 concentration cause the decrease of concentration for all other silicon-bearing species, even for carbon-bearing ones:  $\text{SiC}_2$  – #11 and SiC – #24. Therefore, it seems that SiS molecule controls the silicon chemistry in the examined case. The considerable increase in concentration of sulfur monoxide (SO – #45) is caused by both: an access to sulfur due to decrease of  $n_{\text{CS}}$  and an access to oxygen due to decrease of  $n_{\text{SiO}}$  (SiO – #19). Furthermore, enrichment of the gas in carbon results in increasing concentrations of all molecules composed of only C or carbon and hydrogen. Note, that decreasing of  $\Delta G^\circ$  for NS – #39 (molecule with the second largest difference between  $\Delta G^\circ$  in the NIST and Tsuji databases) would result in much better agreement between corresponding concentrations *only* for this molecule).

As a starting point for the second test we chosen concentrations marked by the red circles in Fig. 3<sup>4</sup>. They are repeated now by black circles in Fig. 4<sup>4</sup>. The order of species is same as in Fig. 1. Red circles in Fig. 4<sup>4</sup> show now the Tsuji concentrations relative to the NIST ones obtained after

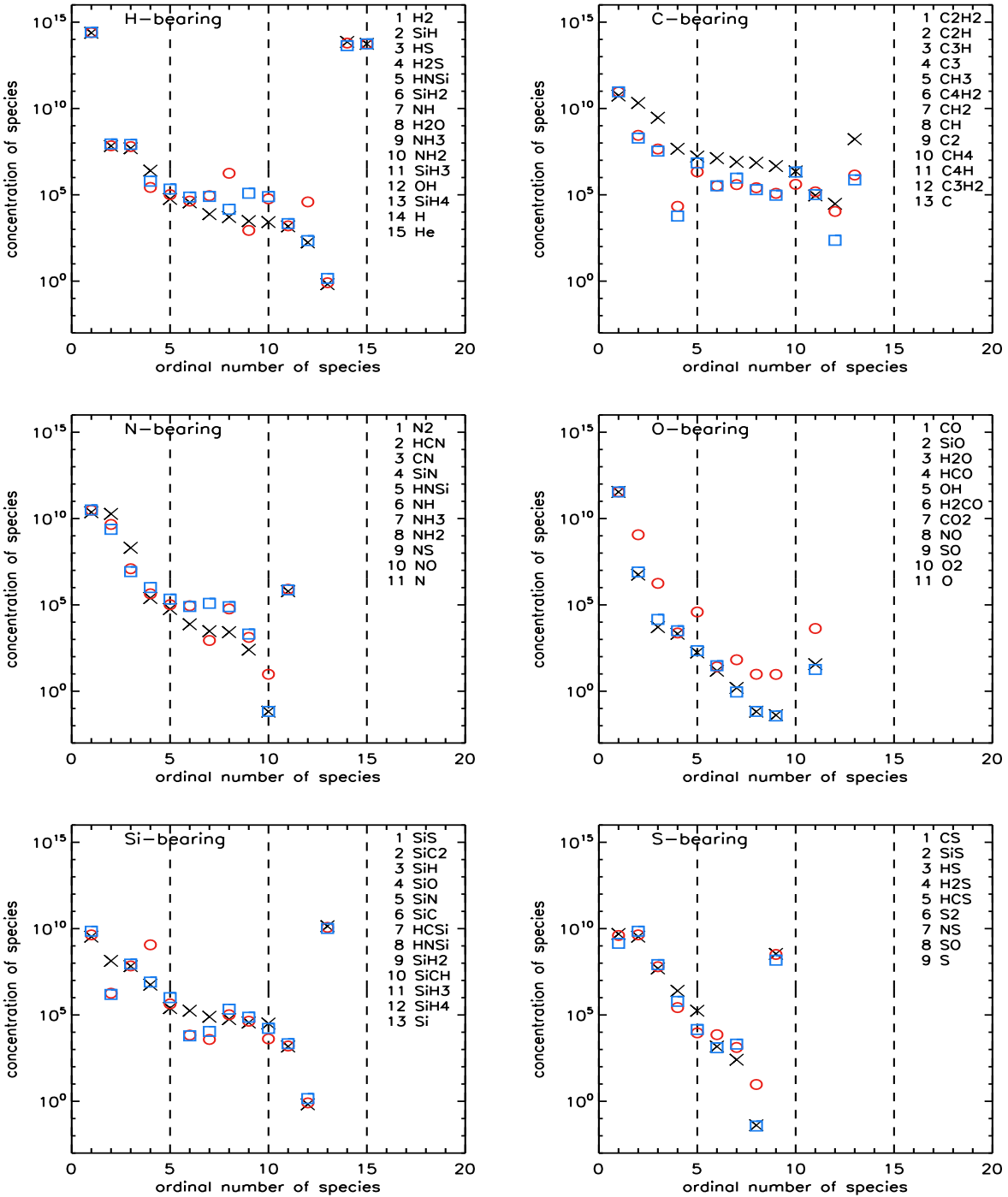


**Fig. 7.** The network balance. Comparison of species concentrations in  $[\text{cm}^{-3}]$  computed for modified WC98 network (case 1 - crosses), which are consistent with TE solution, and for WC98 network (case 2 - circles). Squares mark case similar to case 2, with rate constants updated using data from the UDFA05 database. The concentrations are splitted into H-bearing, C-bearing, N-bearing, O-bearing, Si-bearing, and S-bearing molecules. For each panel we defined the separate ordinal number of species according to decreasing equilibrium concentrations with exception of atom(s) which are shown on the right side of each panel.

additional replacement of  $\Delta G^\circ$ 's by the NIST values for all molecules, which show significant discrepancy in the Gibb's energies (i.e. for CN - #10, SiC<sub>2</sub> - #11, SiH - #12, C<sub>3</sub> - #13, CH<sub>3</sub> - #15, CH<sub>2</sub> - #17, SiN - #23, NH<sub>2</sub> - #35, HCO - #36, and NS - #39 - see Fig. 2 and Table 2). As we can see, changes in  $\Delta G^\circ$ 's for these molecules alter almost only concentrations for these species. The exception is C<sub>3</sub>, where atomic carbon released by

its decreasing abundance (due to the smaller  $\Delta G^\circ$  in the NIST database) is bound also into other carbon-bearing molecules: C<sub>3</sub>H - #9, SiC<sub>2</sub> - #11, C<sub>4</sub>H<sub>2</sub> - #16, C<sub>4</sub>H - #26, and C<sub>3</sub>H<sub>2</sub> - #31.

Finally, we present results, which show how relatively small changes of  $\Delta G^\circ$  for abundant molecule like acetylene (C<sub>2</sub>H<sub>2</sub> - #3) alter the equilibrium abundances of other molecules.  $\Delta G^\circ$  for acetylene from the Tsuji database is *only* about 3.6 [kJ/mol]

smaller than that from NIST (see Table 2). In Fig. 5<sup>4</sup> we present the ratio between the Tsuji and NIST equilibrium concentrations by black circles, while red circles show these ratios computed with  $\Delta G^\circ$  replaced only for acetylene by the larger value from the NIST. As we can see, even so small change in  $\Delta G^\circ$  for this parent and abundant molecule alter significantly the obtained concentrations for almost all other species. With larger  $\Delta G^\circ$  for acetylene more carbon is used for formation of this molecule and therefore concentration of other C-bearing molecules are significantly decreased. This affects also concentrations of other species. In case of silicon-bearing molecules all silicon released from  $\text{SiC}_2$  is bounded into  $\text{SiS}$  and  $\text{SiO}$ . The less sensitive to the change of  $\Delta G^\circ$  for acetylene turned out to be such molecules as:  $\text{SiH}$  – #12,  $\text{HCS}$  – #25,  $\text{SiH}_2$  – #29,  $\text{HCO}$  – #36,  $\text{SiH}_3$  – #37,  $\text{H}_2\text{CO}$  – #41, and  $\text{SiH}_4$  – #43.

### 3. Test of chemical codes: The chemical kinetics

In the outer part of the stellar atmospheres one can expect that non-TE effects are becoming more and more important and non-TE methods to determine properly concentrations of chemical species are necessary. We have developed a kinetic code, which can treat time-dependent chemistry and describe here the performed tests. Now, however, instead of using dissociation constants (or equivalently  $\Delta G^\circ$ 's) we need to consider an appropriate reaction network. In this work we consider reaction network of WC98.

#### 3.1. The kinetic code and reaction network

To find molecular concentrations we have to consider all chemical reactions from the given network, which lead to formation and destruction of all molecules under study. The evolution of concentration with time for species X can be written as:

$$\frac{dn_X}{dt} = F_X - D_X, \quad (9)$$

where: the  $F_X$  stands for reactions responsible for production of species X, and  $D_X$  for its destruction. In the developed code the rate equations, defined for each considered reaction, are accumulated. The rate equation describes the rate of disappearance of each of the reactants and on the other hand the appearance rate of each of the products. For example, for reaction  $A + B \rightarrow C + D$  the rate equation is defined as:

$$-\frac{dn_A}{dt} = -\frac{dn_B}{dt} = \frac{dn_C}{dt} = \frac{dn_D}{dt} = k n_A^\gamma n_B^\delta, \quad (10)$$

where:  $n_A$ ,  $n_B$  – are the concentrations of reactants,  $n_C$ ,  $n_D$  – are the concentrations of products, and the parameters  $\gamma$  and  $\delta$  characterise order of reaction with respect to each reactant. These parameters are derived experimentally and their sum determines the reaction order. The coefficient  $k$  in the above equation is known as a reaction rate constant and determines reaction dependence on the temperature. In our model the order of considered reactions was always the same as the reactants number, i.e.  $\gamma$  and  $\delta$  were equal 1.

We search for the steady state solution of the above set of rate equations using DVODE solver for systems of ordinary differential equation written at Lawrence Livermore National Laboratory<sup>5</sup>. DVODE solves the stiff system of differential

equations of first order, just like systems which are often met in the chemical kinetics. The solver must be updated with the subroutine providing the net reaction rates and eventually subroutine providing Jacobian of the system. These two routines are constructed automatically by searching the network for given molecules and preparing set of corresponding rate equations for given range of temperature. The WC98 reaction network used in our study includes 53 species (7 elements and 46 molecules – given in Table 1 and Table 2, respectively). The molecules are composed of six elements: H, C, N, O, Si, and S. In Table 5 of WC98 there are data for 352 reactions. Among them there are 139 reactions in both directions (hereafter "two-way") and 213 reactions which do not have the backward reaction documented (hereafter "one-way", marked by " $\leftrightarrow$ " in their table). However there are some miss printings in this table:

1. The "two-way" reaction number 53 ( $\text{H}_2 + \text{N}_2 \rightarrow \text{NH} + \text{NH}$ ) has rate constant documented as being zero. We computed this missing rate constant (by method described below - see Eqs. 12 and 13) using equilibrium constant and the rate constant for its backward reaction (i.e. for reaction number 269:  $\text{NH} + \text{NH} \rightarrow \text{H}_2 + \text{N}_2$ ). Note, however, that such approach causes that reaction 269 must be treated as "one-way" process. After this change number of "one-way" reactions in network increased by one to 214, while number of "two-way" reactions decreased to 137;
2. The reaction number 78 ( $\text{C} + \text{NS} \rightarrow \text{CS} + \text{N}$ ) is indicated as a "two-way" reaction (there is no " $\leftrightarrow$ " in the table), but this reaction does not have backward reaction documented and, in fact, should be treated as "one-way" process. This change caused that number of "one-way" reactions increased to 215, while the number of "two-way" reactions decreased to 136;
3. The reaction number 217 ( $\text{S} + \text{N}_2 \rightarrow \text{S} + \text{NS}$ ) is incorrect. It seems that the correct version of this reaction is:  $\text{S} + \text{N}_2 \rightarrow \text{N} + \text{NS}$ . However, such reaction is already present in the network, therefore we simply deleted reaction number 217 from the list. This way, number of "one-way" reactions decreased by one to 214;
4. The correct version of reaction 279 ( $\text{SiH} + \text{NO} \rightarrow \text{SiO} + \text{H}$ ) should be  $\text{SiH} + \text{NO} \rightarrow \text{SiO} + \text{NH}$ . This does not change the statistics of reactions.

In summary, we have 564 reactions in the network according to Table 5 of WC98: 214 in "one-way" + 214 backward – determined as described below + 136 "two-way" reactions.

The rate constants for forward and backward reactions documented in Table 5 of WC98 were computed via equation in Arrhenius form:

$$k_{f,b} = A \left( \frac{T}{300} \right)^\beta \exp \left( -\frac{E_a}{T} \right), \quad (11)$$

where:  $k_f$  and  $k_b$  are the rate constants of forward and backward reactions, respectively,  $A$ ,  $\beta$ , and  $E_a$  are the Arrhenius parameters given in that table. In case of missing backward reactions, WC98 calculated the backward rate constant  $k_b$  from the thermodynamics of the reaction (see Eq. 4 in WC98). In our computations the backward rate constant  $k_b$  for specific reaction and given temperature was derived from the ratio of rate constant for forward reaction, and the reaction equilibrium constant  $K_r$ , i.e.:

$$k_b = k_f / K_r. \quad (12)$$

On the other hand, the equilibrium constant for given reaction can be obtained from the ratio of equilibrium

<sup>5</sup> <http://www.llnl.gov/CASC/odepack/>



concentrations for products and reactants. For example, for reaction  $AB + C \rightarrow AC + B$  the corresponding equilibrium constant is given by:

$$K_r = \frac{n_{AC}n_B}{n_{AB}n_C}, \quad (13)$$

where:  $n_{AB}$ ,  $n_C$ ,  $n_{AC}$ ,  $n_B$  – equilibrium concentrations of reactants and products, respectively. Therefore after inserting  $K_r$  given by Eq. (13) into Eq. (12) we have:

$$k_b = k_f \frac{n_{AB}n_C}{n_{AC}n_B}. \quad (14)$$

Thus, by computing *missing* backward rate constants, we have modified the original network of WC98 and use it to test our kinetic code.

### 3.2. Comparison of TE concentrations derived with WC98 and UDFA05 reaction networks

The chemical timescales in the dense and warm part of the envelope are very short, so the concentrations of species should reach the steady state values very quickly. Therefore, to test our kinetic code we decided to reproduce the equilibrium concentrations of the 53 species discussed above. In such case, as an input to the code we need the initial concentrations of elements only (values are taken from Table 1), the total gas density and its temperature (again we have adopted physical conditions specified in the 1<sup>st</sup> entry of Table 2 in WC98).

To test our chemical kinetic code we have adopted rate constants only for the forward reactions<sup>6</sup> (282 = 136/2+214 – the network of WC98 requires the rate equations for 564 reactions) and we have computed the rate constants for all (282) backward reactions according to the method described above (hereafter case 1). As expected, in this case our code reproduces the WC98 equilibrium concentrations. The results are marked as crosses in Fig. 6. The species (except atoms collected at the right side of the plot) are plotted in order of decreasing abundances. In addition, we have tested stability of our code by assuming that initial chemical composition of all species is equal to that at the thermodynamical equilibrium for the considered conditions. No changes in the species concentrations were seen after very long time ( $10^8$  sec). Therefore, for further computations we used the equilibrium concentrations as an input to our code (for its faster convergence). Note that the results are the same when we start with a purely atomic gas.

In the next test (hereafter case 2) we took all rate constants available in the WC98 network (i.e. 350 = 214 + 136 - see the previous subsection) and computed the rate constants only for the missing (214) backward reactions by using NIST thermochemical data (in fact, this approach is the same as described by WC98). The results are presented in Fig. 6 as circles. It is seen, that the present steady state differs from the thermodynamical equilibrium concentrations (case 1). More detailed comparison for all species, which belong to a given family (molecules containing element: H, C, N, O, Si, and S, respectively) are presented in six panels in Fig. 7<sup>4</sup> as circles: going from the left to right and from the top to bottom for:

<sup>6</sup> As a forward reaction, among reactions with rate constants given for both directions, we chose the reaction with more precise rate constant i.e. first when Arrhenius parameter  $\beta$  (see Eq. 11) is different from zero. If  $\beta = 0$  for both reactions, we took reaction with smaller Arrhenius parameter  $E_a$ . In case of reactions without the backward rate constants we treat all of them as a forward reactions.

H, C, N, O, Si, and S. For each panel we defined the separate ordinal number of species according to decreasing equilibrium concentrations with exception of atom(s) which are shown on the right side of each panel.

The inconsistency in species abundances is rather high and only fifteen species differ less than 30 % (i.e. He, CO, H<sub>2</sub>, SiH, SiH<sub>3</sub>, S, HCO, Si, H, CS, SiH<sub>2</sub>, SiH<sub>4</sub>, HS, SiS, N<sub>2</sub>, and N). The highest differences are seen for oxygen-based molecules. Only formyl (HCO) and the most abundant among O-bearing molecules – carbon monoxide (CO) are in relatively good agreement with the corresponding equilibrium concentrations. Concentrations of other molecules (i.e. SiO, H<sub>2</sub>O, OH, H<sub>2</sub>CO, CO<sub>2</sub>, NO, SO, and O<sub>2</sub>) are far from equilibrium values.

The WC98 network was created on the basis of the RATE95 database (Millar et al. 1997). The discrepancies present in the above results encourage us to update the rate constants using the UDFA05 database (Woodall et al. 2006). We found that 162 reactions among 564 have now the new values of the rate constants. We performed the same test as in case 2 (i.e. only missing backward rates were computed using Eq. 14) with the reaction network updated using the UDFA05 database. The results are presented as squares in Fig. 6, and the family splitting in this case is shown in Fig. 7<sup>4</sup> also by squares.

The agreement with the equilibrium state for oxygen-bearing molecules now is much better. However, the discrepancies in abundances of carbon-bearing molecules are still present. Moreover, the differences with equilibrium results for nitrogen-bearing molecules are even higher.

The most likely source of inconsistency is the problem with the determination of reaction rate constants for the silicon- and sulfur-bearing species. WC98 estimated the rate constants for these reactions from similar reactions involving covalent species, i.e. oxygen for sulfur and carbon for silicon (see comments in Table 5 of WC98). When this group of reactions was excluded from the studied network, the abundances of carbon-bearing and oxygen-bearing molecules became more consistent with LTE results. However, the results for nitrogen-bearing species are still unsatisfactory and additional work on the chemical network extension is needed.

## 4. Conclusions

In this paper we have performed tests of our chemical (equilibrium and kinetic) codes with the aim to use them during self-consistent modelling of dynamics and chemistry in outflows from C-rich AGB stars.

The LTE molecular distribution at the base of the wind is needed as the boundary condition to determine chemical composition in the circumstellar envelope of the AGB star. In such LTE calculations it is necessary to keep in mind the possible influence of the different sets of equilibrium dissociation constants on the species concentration. Analysis of the conducted test calculations shows that, fortunately, such influence for not abundant molecules is rather small. However, for more abundant species the influence is crucial and the used sets of equilibrium dissociation constants should be carefully selected and checked. In particular, our calculations have shown that the NIST database reproduce well the WC98 equilibrium concentrations, while agreement between WC98 and Tsuji is much worse.

Steady state solution obtained with kinetic code for WC98 reaction network is different from the thermodynamical equilibrium solution. This would affect the full time-dependent

radiative-hydrodynamic computations of the inner wind. Note that CN and C<sub>2</sub> molecules, important for the opacity computations in the atmosphere of carbon rich star, are underabundant by more than one order of magnitude in comparison to equilibrium concentration (see Fig.6). Our kinetic computations also show the strong overabundance of oxygen-bearing molecules (especially of SiO, H<sub>2</sub>O, and OH) in comparison to the LTE approach. It would be interesting to investigate how these overabundances influenced the final results of the inner wind studies by Willacy & Cherchneff (1998) and Cherchneff (2006).

To make both, LTE and kinetic, models consistent we propose to replace all reaction rates in backward direction<sup>7</sup> by reaction rates computed from forward reactions with usage of thermochemical data. Then, in the limit of high density and temperature (i.e. when chemical timescales are much shorter than dynamical timescales) the kinetic steady state solution approach the local thermodynamical equilibrium.

Observations (Tsuji et al. 1973) and the astrochemical modelling (WC98, Cherchneff 2006) are showing that the base of inner wind in AGBs is a region of active chemistry. Therefore, chemical network, which may be used to investigate the composition of this region should include extended set of chemical reactions such as neutral–neutral involving metals and photochemistry induced by the stellar radiation field. This will be direction of our future studies.

*Acknowledgements.* We are very indebted to the referee Karen Willacy for providing us with the original Gibb's free energies used in WC98 and for comments which allowed us to improve the manuscript.

This work has been partly supported by grants 2.P03D 017.25 and 1.P03D.010.29 of the Polish State Committee for Scientific Research.

## References

- Asplund, M., Grevesse, N., & Sauval, A. J. 2005, ASPC, 336, (A05)  
 Cherchneff, I. 2006, A&A, 456, 1001  
 Glassgold, A. E. 1996, ARA&A, 34, 241  
 Grevesse, N. & Sauval, A. J. 1998, SSRv, 85, 161, (GS98)  
 Millar, T. J. 2003, Molecule and Grain Formation in 'Asymptotic Giant Branch Stars' eds. H J Habing & H Olofsson, Springer, NY, 247  
 Millar, T. J., Farquhar, P. R. A., & Willacy, K. 1997, A&AS, 121, 139  
 Olofsson, H. 2006, Rev. Mod. Astron., 19, 75  
 Pulecka, M., Schmidt, M., Shematovich, V., & Szczerba, R. 2005a, dmu.conf, 457  
 Pulecka, M., Schmidt, M., Shematovich, V., & Szczerba, R. 2005b, IAUS, 231, 71  
 Russell, H. N. 1934, ApJ, 79, 317  
 Tsuji, T. 1973, A&A, 23, 411  
 Tsuji, T., Ohnaka, K., Aoki, W., & Yamamura, I. 1973, A&A, 320, L1  
 Willacy, K. & Cherchneff, I. 1998, A&A, 330, 676, (WC98)  
 Woodall, J., Agundez, M., Markwick-Kemper, A. J., & Millar, T. J. 2006, A&A, submitted

---

<sup>7</sup> see footnote 6